Tracking a large vortex at a tidal power site

Philippe Mercier, and Sylvain S. Guillou

Abstract—**Tidal turbines are sensitive to the high turbulence of tidal flows. Large and intense vortices are generated at the seabed and cause extreme loads, fatigue damage and degraded power production. Thus, these vortices must be characterised prior to the turbine installation. The vortex characteristics are strongly affected by the seabed macro-roughness (rocks, faults) that induces spatial variations of the flow characteristics at a local scale. Numerical simulations, that cover large areas, are suited to catch these spatial variations. The ability of Large Eddy Simulations (LES) to simulate turbulent motions has been validated at a tidal power site. The most critical flow conditions can be identified. However, LES are computationally expensive, which reduces their spatial and temporal coverages to a few square kilometers and a few tens of minutes. This limits the possibility of a comprehensive prediction of the most intense turbulent events occurring at a tidal power site. Rather than trying to fully characterise a given tidal power site, this work aims at identifying the physical processes leading to extreme turbulent events. To do so, the vortices must be detected and tracked individually, to understand their generation process in relation with the local seabed morphology. A few vortices are detected and extreme flow variations are observed in their vicinity. This confirms the interest of the method for an easy detection of the most troublesome vortices and the seabed morphologies that generate them.**

Index Terms—**Tidal flows, Turbulence, Numerical simulation, Seabed roughness**

I. Introduction

THE tidal industry is ramping up from the test of full-size prototypes towards the installation of commercial farms. Several pilot farms are in development (Normandie Hydrolienne project, FloWatt project, Phares project) or already operating (Meygen). One of the main uncertainty for the growth of the tidal sector is the durability of the tidal devices, that are exposed to a harsh environment. Notably, tidal flow are highly turbulent, which affects the turbine production and wakes, and induces extreme and fatigue loads [1], [2].

The turbulence intensity of tidal flows is affected by the waves, the wind, the seabed morphology and the presence of turbines. The impact of turbulence at a given site can be assessed through acoustic Doppler current profiler (ADCP) measurements. However, ADCP devices only provide a vertical profile at their location, which is not sufficient to capture the fine spatial variations of the flow characteristics [3].

This work is currently funded by the European Union in the frame of the France Channel England INTERREG project TIGER.

P. Mercier and S.S. Guillou are with the Applied Science Laboratory of Cherbourg (LUSAC), University of Caen Normandy, 60 rue Max-Pol Fouchet, 50100 Cherbourg-en-Cotentin (e-mail: philippe.mercier@unicaen.fr, sylvain.guillou@unicaen.fr).

Digital Object Identifier:
https://doi.org/10.36688/ewtec-2023-339

Fig. 1. Boil at the surface of Raz Blanchard. Courtesy Lucille Furgerot.

In contrast, numerical simulations cover wide areas. Large-eddy simulations (LES) reproduce the turbulent motions [4]–[6] and can help identifying the best locations for the turbine installation [7].

Fig. 2. Location of the Paimpol-Bréhat tidal test site.

However, LES are computationally expensive, which constraints the flow conditions that can be studied. Also, the result interpretation is time-consuming due to the high volume of data to be treated. For these reasons, being able to predict the areas where intense vortices are likely to be detrimental to tidal turbines, based only on the observation of the seabed morphology and the characteristics of the flow available from regional Reynolds averaged Navier-Stokes simulations (flow direction and intensity), would be a big

improvement for a more efficient turbine positioning. Reaching this goal requires a better understanding of the vortex dynamics in powerful tidal flows. The present contribution focuses on the turbulent vortices generated at the seabed. These vortices are found to be intense and to sustain over long distances. Some of them are observed to reach the sea surface (see Figure 1) [8]. The physical processes at stake for their generation and time evolution are complex [9], [10] and highly dependent on the seabed morphology [11]–[13]. This study concerns the Paimpol-Bréhat tidal test site Figure 2. First, the simulation method, setup and overall results are presented, as well as a description of a vortex detection method. Then, some vortices are detected on the whole simulation domain and on targeted areas. Finally, the insights of this simulation and the benefits of the vortex detection method are discussed.

II. Methods

A. Numerical setup

The numerical model is based on the lattice Boltzmann method (LBM) implemented in the open-source C++ library Palabos [14]. LBM is an unsteady numerical flow simulation method based on the resolution of the Boltzmann equation [15]. Coupled with the large-eddy simulation (LES) [16], it is suited for the simulation of turbulent flows. Its low numerical dissipation allows an accurate simulation of turbulent motions [17]. Due to the simplicity of its execution, it handles heavy meshes of complex geometry on massively parallel computations at a low computational cost, relative to more classical Navier-Stokes formulations [18].

The study area is located in the Paimpol-Bréhat site in France (Figure 2). The flow velocity reaches 3 $m.s^{-1}$ [19] and the site is equipped with facilities that make it a good test site work full scale tidal turbine prototypes. The simulation domain measures 1091 m in length and 409 m in width, with a depth ranging from 30 m to 55 m. The seabed morphology is known from a bathymetry of resolution 1 m. The simulation domain is discretised into a Cartesian mesh of 330 millions of nodes with a 0.33 m resolution near the seabed and a 0.66 m resolution near the sea surface.

The seabed is modelled with a no-slip boundary condition [20]. The collision model is based on the Bhatnagar, Gross and Krook model [15] with an increased numerical stability based on a regularisation procedure [21]. The subgrid scale model is a LBM version of the Smagorinsky model [22], using a Smagorinsky constant of 0.14. The sea surface is modelled by a free slip boundary condition and the lateral boundary condition by a Dirichlet condition [23]. These boundaries are supplemented with 2 m thick zones of increased viscosity. The domain is periodic in the longitudinal direction and a uniform force sustains the flow at an average of 2 $m.s^{-1}$. This model has been used in several studies [6], [24], [25] and validated against in site measurements in the Raz Blanchard [5] and at Paimpol-Bréhat tidal site [7]. A global view of the simulation domain and cross-sections of instantaneous longitudinal velocity are shown in Figure 3.

B. Average quantities

The simulation has been validated against in site measurements in a previous work [7]. Some time-averaged results are shown in Figure 4a (average longitudinal velocity) and Figure 4b (longitudinal velocity variance), on a horizontal plane at a 20 m depth. Figure 4a brings to light longitudinal streaks of underspeed (around 2.0 $m.s^{-1}$) and overspeed (around 2.5 $m.s^{-1}$). In Figure 4b similar streaks are observed on the average longitudinal velocity variance, that reflects the flow turbulence. The streaks of overspeed are situated at the location of streaks of low turbulence and vice versa. These results are consistent with previous work [6].

C. Vortex detection method

Usually, vortex visualisations are based on isosurfaces of quantities such as pressure, vorticity, λ_2 criterion [26] or Q criterion [27]. These visualisations are suited for the interpretation of the dynamics of turbulent motions by humans. However, they are based on the choice of thresholds that depend on the flow characteristics. The optimal thresholds may vary spatially within a given flow. A high number of vortices may complicate the identification of individual vortices due to their overlapping. Finally, the numerical identification of an individual vortex is complex on parallel computation, because it relies on non-local operations. For these reasons, these isosurface visualisations are highly time consuming and difficult to automate. Therefore, the identification of vortices by their cores can be more appropriate. Vortices usually take elongated shapes that can be identified by their central line, for example by detecting helicity lines [28] or vorticity maxima [29]. Notably, the predictor-corrector method [30] is based on the tracking of vorticity lines and pressure minima. The later method is adapted here to the tracking of vorticity lines and λ_2 minima.

The tracking method consists of four steps:

1) Detection of local minima of λ_2 criterion.
2) Growing of the core lines following vorticity lines and applying a correction by the minimum of λ_2 criterion.
3) The core line growing stops when a shutoff parameter is reached (contact with another core line, contact with a wall, low vortex intensity).
4) The core lines are filtered, removing the smallest and the least powerful ones.

At step one, the value of the λ_2 criterion of each mesh node is compared to all its neighbouring nodes. If no neighbouring node has a higher value of λ_2, the mesh node is tagged as a local minimum of λ_2, from which the core lines will be grown. At step two, the core lines are grown from local minima of λ_2. The neighbouring nodes that are in the direction of the vorticity vector are pre-selected (prediction step) and among them the node having the minimum value of λ_2 is added to the core line. This process is repeated from this node until step three, when the selected node already belongs to a core line, belongs to a solid wall, or if the vortex intensity is low. This last criteria is

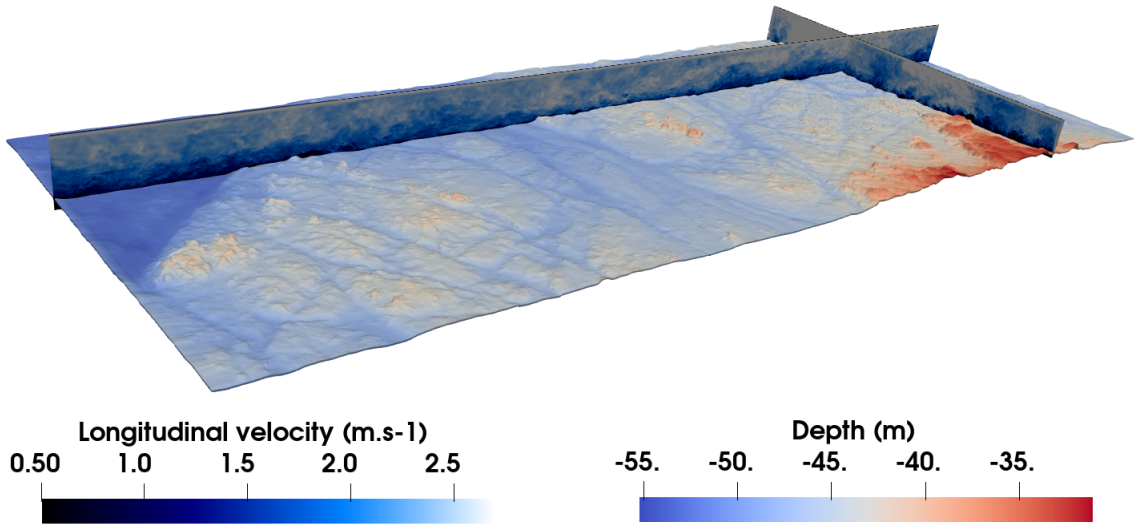

Fig. 3. Instantaneous longitudinal velocity.

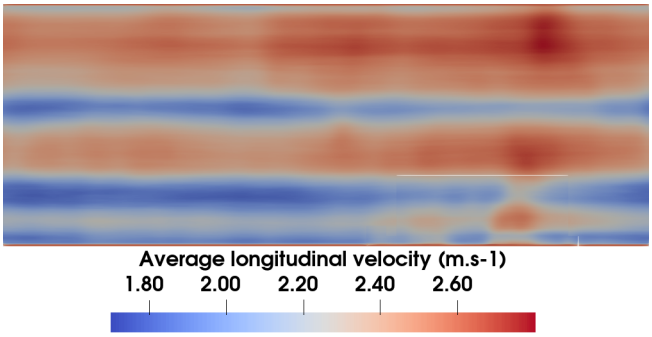

(a) Average longitudinal velocity.

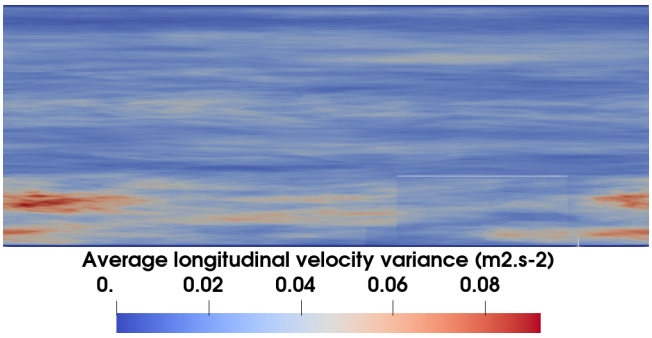

(b) Longitudinal velocity variance.

Fig. 4. Average longitudinal velocity and velocity variance at a 20 m depth.

evaluated by checking if the vorticity of the neighbouring nodes is not collinear to the vorticity of the core line node. These three steps are performed during the calculation and only involve local calculations, which ensures a low computational cost. The fourth step is performed in post-processing. The shortest and the least powerful vortices are removed to capture only the relevant physical processes.

III. Results

A. Large spatial coverage vortex detection

The vortex detection method is first applied on the whole simulation domain, as in Figure 5. The vortices are coloured by their altitude, with hot colours in the upper part of the water column and cold colours in the lower part.

Large vortices are identified as typical horseshoe structures (see zoom number 2, for example). These structures are organised in trails, with successions of several large vortices of similar shapes and altitudes. Some of these trails are situated just downstream of large rocks (see zoom number 3). Some other trails cannot be obviously related to a seabed asperity (see zoom number 1), or possibly to a seabed asperity situated far upstream (see zoom number 2).

In some areas, such as Zone A and Zone B, a lot of small vortices are observed downstream large rocks. These vortices do not organise in trails, they stick close to the seabed and do not sustain over long distances. No large vortices are identified among the numerous small vortices.

The seabed of the simulation domain is crossed by faults and cracks. These asperities are not associated with vortices in a clear way, by contrast with rocky asperities.

B. Focus on individual vortices

The identification of areas where large and intense vortices are generated paves the way to their detailed study. In Figure 6 two large vortices are observed in the vortex trail identified in the Zoom 3 area in Figure 5. These two vortices are similar in dimensions to the large rock that is suspected to have generated them, with an approximate 20 m to 30 m extend. They have a typical horseshoe shape and expand over around 20 m in depth.

To assess the impact of this type of turbulent motions on potential tidal turbines, their influence on the flow at a local scale is visualised over a volume representative of standard dimension turbines. In Figure 7, a large horseshoe vortex is reaching a visualisation disk of 18 m diameter representative of a 1.5 MW turbine. The disk is coloured by the longitudinal velocity. At the point where the vortex crosses the disk, a very strong gradient of longitudinal velocity forms. The

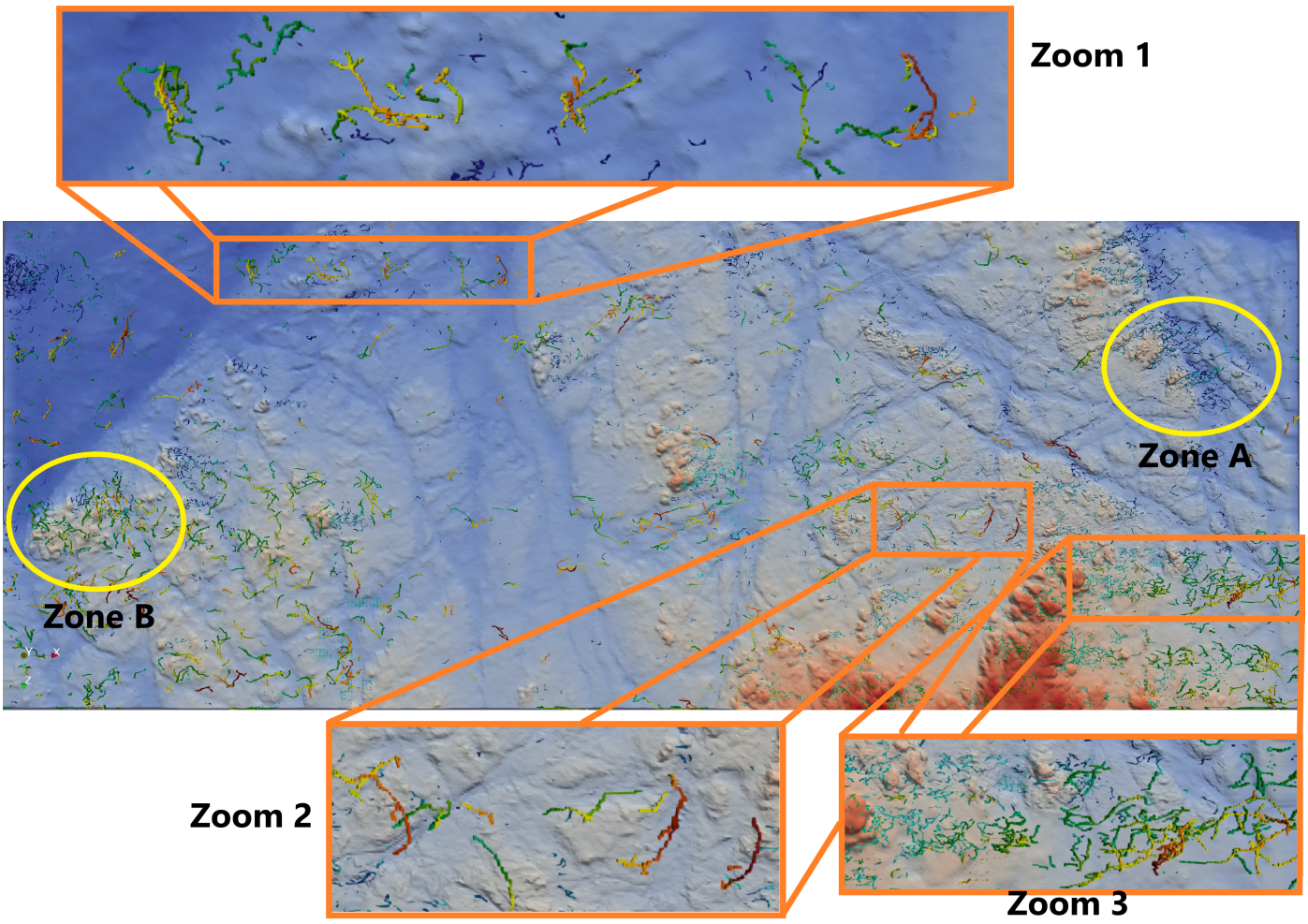

Fig. 5. Overview vortex visualisation.

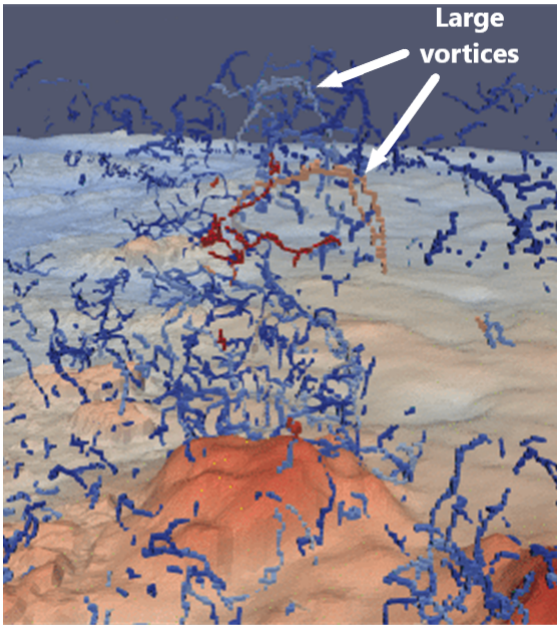

Fig. 6. Two large vortices identified in the wake of a large rock (see Zoom 3 in Figure 5).

longitudinal velocity varies from 1.8 m.S^{-1} to 2.9 m.s^{-1} in a few meters.

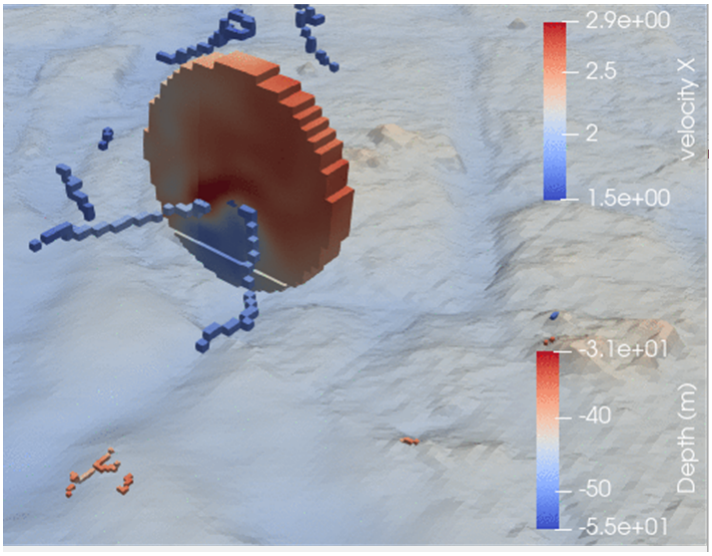

Fig. 7. Impact of a large vortice on a fictive turbine.

IV. Discussion and conclusion

High resolution numerical simulations of environmental flows are rare in the literature. The results of the present work bear similarity with previous works, which strengthen their findings. However, the differences in the seabed morphology have a notice-

able effect on the flow characteristics. The use of a vortex detection method helps understanding the flow dynamics.

The trails of underspeed and overspeed observed in this simulation are consistent with previous simulations [6], [7], [24]. The present contributions tends to confirm the association of underspeed trails with high turbulence and the association of overspeed trails with low turbulence, which is already described in the literature [31]–[33]. This phenomenon is essential for an appropriate turbine positioning. Indeed, the distance between trails of underspeed and overspeed is of the order of a hundred meters, which is a very fine scale compared to tidal resource assessment maps. Also, the trails of underspeed are associated with a higher turbulence, which reinforce the need to avoid placing turbines at these places.

The detection of numerous successions of large vortices contrasts with previous simulations for which only few and isolated large vortices were detected [5], [6]. Also, the turbulence generators in the Raz Blanchard tidal power site were mostly identified as seabed asperities elongated in the direction transverse to the flow [6]. This contrasts with the present work, where the turbulent structures are mostly present downstream of large and sharp rocks. One possible interpretation for this lies on the differences in the bathymetry morphology. In the studied part of the Raz Blanchard [6], the bathymetry indicates a rough seabed and the largest seabed asperities are faults and cracks. There are no large rocky obstacles. In the present work, the seabed is relatively smooth, but dotted with large, steep and isolated rocks. Thus, the flow dynamics at the Paimpol-Bréhat site could be regarded as a superposition of independent obstacle wakes, whereas the flow dynamics at the Raz Blanchard site is closer to a fully rough wall flow, in which the unsteady motions are modelled by the combination of various seabed asperities.

The vortex detection method is suited for the identification of large turbulent motions. It simplifies the capture of the most intense coherent structures, that have a strong impact on the flow characteristics. The filtering of smaller and less powerful vortices clarifies the global view of the flow and enable targeting the areas of interest within the simulation domain. The method helped detecting a highly energetic vortex inducing a very high velocity gradient on a potential turbine. The detection of such an exceptional turbulent event is crucial to avoid placing a turbine in a trajectory where intense turbulent vortices are likely to run. In a previous study of the same tidal power site [7], a random arrangement of probes was not able to detect a vortex as intense as the one detected in the present study.

Acknowledgement

This work is funded by the Tidal Stream Industry Energiser project (TIGER), co-financed by the European Regional Development Fund through the INTERREG France (Channel) England Programme. We are grateful to the CRIANN (”Centre Régional Informatique et d’Applications Numériques de Normandie”) for providing computational means, EDF, SEENEOH and Energie de la Lune for providing bathymetric data and EDF for providing ADCP measurement data.

References

[1] B. Gaurier, P. Druault, M. Ikhennicheu, and G. Germain, “Experimental analysis of the shear flow effect on tidal turbine blade root force from three-dimensional mean flow reconstruction,” *Philosophical Transactions of the Royal Society A*, vol. 378, no. 20200001, 2020. [Online]. Available: http://dx.doi.org/10.1098/rsta.2020.0001 I

[2] B. Gaurier, M. Ikhennicheu, G. Germain, and P. Druault, “Experimental study of bathymetry generated turbulence on tidal turbine behaviour,” *Renewable Energy*, vol. 156, pp. 1158–1170, 2020. [Online]. Available: https://doi.org/10.1016/j.renene.2020.04.102 I

[3] M. Togneri and I. Masters, “Micrositing variability and mean flow scaling for marine turbulence in ramsey sound,” *Journal of Ocean Engineering and Marine Energy*, vol. 2, pp. 35–46, 2016. [Online]. Available: https://doi.org/10.1007/s40722-015-0036-0 I

[4] A. Bourgoin, S. Guillou, J. Thiébot, and R. Ata, “Turbulence characterization at a tidal energy site using large-eddy simulations: case of the Alderney Race,” *Philosophical Transactions of the Royal Society A*, vol. 378, no. 20190499, 2020. [Online]. Available: https://doi.org/10.1098/rsta.2019.0499 I

[5] P. Mercier, M. Grondeau, S. Guillou, J. Thiébot, and E. Poizot, “Numerical study of the turbulent eddies generated by the seabed roughness. Case study at a tidal power site,” *Applied Ocean Research*, vol. 97, no. 102082, 2020. [Online]. Available: https://doi.org/10.1016/j.apor.2020.102082 I, II-A, IV

[6] P. Mercier and S. Guillou, “The impact of the seabed morphology on turbulence generation in a strong tidal stream,” *Physics of Fluids*, vol. 33, no. 055125, 2021. [Online]. Available: https://doi.org/10.1063/5.0047791 I, II-A, II-B, IV

[7] ——, “Spatial and temporal variations of the flow characteristics at a tidal stream power site: A high-resolution numerical study,” *Energy Conversion and Management*, vol. 269, no. 116123, 2022. [Online]. Available: https://doi.org/10.1016/j.enconman.2022.116123 I, II-A, II-B, IV

[8] J. Slingsby, B. Scott, L. Kregting, J. McIlvenny, J. Wilson, A. Couto, D. Roos, M. Yanez, and B. Williamson, “Surface characterisation of kolk-boils within tidal stream environments using uav imagery,” *Journal of Marine Science and Engineering*, vol. 9, no. 484, 2021. [Online]. Available: https://doi.org/10.3390/jmse9050484 I

[9] P. Mercier, M. Ikhennicheu, S. Guillou, G. Germain, E. Poizot, M. Grondeau, J. Thiébot, and P. Druault, “The merging of Kelvin–Helmholtz vortices into large coherent flow structures in a high Reynolds number flow past a wall-mounted square cylinder,” *Ocean Engineering*, vol. 204, no. 107274, 2020. [Online]. Available: https://doi.org/10.1016/j.oceaneng.2020.107274 I

[10] M. Ikhennicheu, G. Germain, P. Druault, and B. Gaurier, “Experimental study of coherent flow structures past a wall-mounted square cylinder,” *Ocean Engineering*, vol. 182, pp. 137–146, 2019. [Online]. Available: https://doi.org/10.1016/j.oceaneng.2019.04.043 I

[11] M. Ikhennicheu, B. Gaurier, P. Druault, and G. Germain, “Experimental analysis of the floor inclination effect on the turbulent wake developing behind a wall mounted cube,” *European Journal of Mechanics - B Fluids*, vol. 72, pp. 340–352, 2018. [Online]. Available: https://doi.org/10.1016/j.euromechflu.2018.07.003 I

[12] M. Ikhennicheu, G. Germain, P. Druault, and B. Gaurier, “Experimental investigation of the turbulent wake past realistic seabed elements for velocity variations characterisation in the water column,” *International Journal of Heat and Fluid Flow*, vol. 78, no. 108426, 2019. [Online]. Available: https://doi.org/10.1016/j.ijheatfluidflow.2019.108426 I

[13] M. Ikhennicheu, P. Druault, B. Gaurier, and G. Germain, “Turbulent kinetic energy budget in a wall-mounted cylinder wake using PIV measurements,” *Ocean Engineering*, vol. 210, no. 107582, 2020. [Online]. Available: https://doi.org/10.1016/j.oceaneng.2020.107582 I

[14] J. Latt, O. Malaspinas, D. Kontaxakis, A. Parmigiani, D. Lagrava, F. Brogi, M. B. Belgacem, Y. Thorimbert, S. Leclaire, S. Li, F. Marson, J. Lemus, C. Kotsalos, R. Conradin, C. Coreixas, R. Petkantchin, F. Raynaud, J. Beny, and B. Chopard, “Palabos:

Parallel lattice boltzmann solver," *Computers & Mathematics with Applications*, 2020. II-A

[15] P. Bhatnagar, E. Gross, and M. Krook, "A model for collision processes in gases," *Physical Review*, vol. 94, no. 3, 1954. [Online]. Available: http://dx.doi.org/10.1103/PhysRev.94.511 II-A, II-A

[16] J. Smagorinsky, "General circulation experiments with the primitive equations," *Monthly Weather Review*, vol. 91, no. 3, pp. 99–164, 1963. [Online]. Available: https://doi.org/10.1175/1520-0493(1963)091⟨0099:GCEWTP⟩2.3.CO;2 II-A

[17] S. Marié, D. Ricot, and P. Sagaut, "Comparison between lattice boltzmann method and navier-stokes high order schemes for computational aeroacousitcs," *Journal of Computational Physics*, vol. 228, pp. 1056–1070, 2009. [Online]. Available: https://doi.org/10.1016/j.jcp.2008.10.021 II-A

[18] S. Succi, E. Foti, and F. Higuera, "Three-dimensional flows in complex geometries with the lattice Boltzmann method." *Europhysics Letters*, pp. 433–438, 1989. [Online]. Available: https://doi.org/10.1209/0295-5075/10/5/008 II-A

[19] N. Guillou, S. Neill, and P. Robins, "Characterising the tidal stream power resource around france using a high-resolution harmonic database," *Renewable Energy*, vol. 123, pp. 706–718, 2018. [Online]. Available: https://doi.org/10.1016/j.renene.2017.12.033 II-A

[20] M. Bouzidi, M. Firdaouss, and P. Lallemand, "Momentum transfer of a Boltzmann-lattice fluid with boundaries," *Physics of Fluids*, vol. 13, no. 3452, 2001. [Online]. Available: https://doi.org/10.1063/1.1399290 II-A

[21] J. Latt and B. Chopard, "Lattice Boltzmann method with regularized pre-collision distribution functions," *Mathematics and Computers in Simulation*, vol. 72, pp. 165–168, 2006. [Online]. Available: https://doi.org/10.1016/j.matcom.2006.05.017 II-A

[22] O. Malaspinas and P. Sagaut, "Consistent subgrid scale modelling for lattice boltzmann methods," *Journal of Fluid Mechanics*, vol. 700, pp. 514–542, 2012. II-A

[23] Q. Zou and X. He, "On pressure and velocity boundary conditions for the lattice boltzmann bgk model," *Physics of Fluids*, 1997. II-A

[24] P. Mercier, S. Guillou, J. Thiébot, and E. Poizot, "Turbulence characterisation during ebbing and flooding tides in the Raz Blanchard with large eddy simulations," in *Proceedings of the European Wave and Tidal Energy Conference*, ser. European Wave and Tidal Energy Conference Series, no. 2190, 2021. II-A, IV

[25] P. Mercier, M. Thiébaut, S. Guillou, C. Maisondieu, E. Poizot, A. Pieterse, J. Thiébot, J.-F. Filipot, and M. Grondeau, "Turbulence measurements: An assessment of acoustic doppler current profiler accuracy in rough environment," *Ocean Engineering*, vol. 226, no. 108819, 2021. [Online]. Available: https://doi.org/10.1016/j.oceaneng.2021.108819 II-A

[26] J. Jeong and F. Hussain, "On the identification of a vortex," *Journal of Fluid Mechanics*, vol. 285, pp. 69–94, 1995. II-C

[27] J. Hunt, A. Wray, and P. Moin, "Eddies, streams, and convergence zones in turbulent flows," in *Proceedings of the Summer Program 1988*. Center for Turbulence Research, 1988. II-C

[28] Y. Levy, D. Degani, and A. Seginer, "Graphical visualization of vortical flows by means of helicity," *AIAA Journal*, vol. 28, no. 8, pp. 1347–1352, 1990. II-C

[29] R. Strawn, D. Kenwright, and J. Ahmad, "Computer visualization of vortex wake systems," *AIAA Journal*, vol. 37, no. 4, pp. 511–512, 1999. II-C

[30] D. Banks and B. Singer, "A predictor-corrector technique for visualizing unsteady flow," 1995. II-C

[31] J. Gulliver and M. Halverson, "Measurements of large streamwise vortices in an open-channel flow," *Water Resources Research*, vol. 23, pp. 115–123, 1987. [Online]. Available: https://doi.org/10.1029/WR023i001p00115 IV

[32] A. Shvidchenko and G. Pender, "Macroturbulent structure of open-channel flow over gravel beds," *Water Resources Research*, vol. 37, no. 3, 2001. [Online]. Available: https://doi.org/10.1029/2000WR900280 IV

[33] R. Adrian and I. Marusic, "Coherent structures in flow over hydraulic engineering surfaces," *Journal of Hydraulic Research*, vol. 50, pp. 451–464, 2012. [Online]. Available: https://doi.org/10.1080/00221686.2012.729540 IV